ACS APPLIED MATERIALS & INTERFACES

Research Article

www.acsami.org

Multicomponent Inorganic Janus Particles with Controlled Compositions, Morphologies, and Dimensions

Yekaterina L. Lyubarskaya[†] and Alexander A. Shestopalov*[,‡]

[†]Department of Chemistry and [‡]Department of Chemical Engineering, University of Rochester, Rochester, New York 14627, United States

Supporting Information

ABSTRACT: We report a new protocol for the preparation of shape-controlled multicomponent particles comprising metallic (Au and Ti), magnetic (Ni), and oxide (SiO_2, TiO_2) layers. Our method allows for a precise control over the composition, shape, and size and permits fabrication of nonsymmetrical particles, whose opposite sides can be orthogonally functionalized using well-established organosilanes and thiol chemistries. Because of their unique geometries and surface chemistries, these colloids represent ideal materials with which to study nonsymmetrical self-assembly at the meso- and microscales.

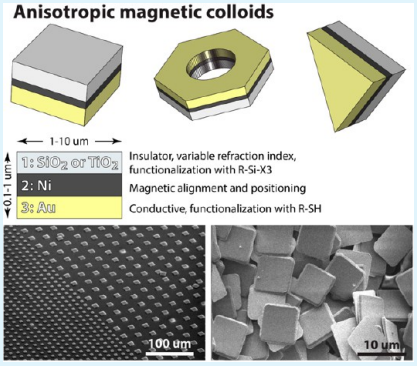

KEYWORDS: *Janus particles, anisotropic colloids, shape-controlled manufacturing, mesoscopic self-assembly, orthogonal functionalization, self-assembled monolayers*

INTRODUCTION

Over the past few years, multicomponent particles have emerged as new colloidal structures with anisotropically distributed properties that have opened up a wide field of unique applications in medicine, biochemistry, optics, physics and chemistry.[1−4] For example, two-faced Janus particles (JPs) have been used as unique nanosensors and nanoprobes,[5−9] and as efficient microscopic mixers and emulsifiers.[2,3] Bicolored anisotropic colloids have been applied in switchable devices and electronic displays;[10] while small nanoscopic multicomponent particles have been proposed for applications in targeted drug delivery and advanced bioimaging.[11−13] Shape-controlled anisotropic colloids functionalized with complementary organic or biological molecules have been suggested as attractive building blocks for new types of self-assembled materials.[13−19] The macroscopic parameters of such self-assembled materials strongly depend on the geometrical, physical, and chemical properties of their elemental components, making anisotropic multicomponent particles ideal candidates for tunable self-assembled aggregates with unique physical and optical properties and potential applications in photonics and electronics.

The synthesis of such particles, however, remains a challenging problem. Usually, such colloids are prepared from the corresponding monocomponent units via different desymmetrization procedures, such as techniques based on toposelective surface modification,[12,14,20−30] template-directed self-assembly,[31−34] controlled phase separation,[35−40] and controlled surface nucleation and growth.[41−45] None of these methods, however, provide access to inorganic colloids with precisely controlled geometry, mainly because the majority of the solution-based methods for meso- and microcolloids yield only simple spherical particles. Two-dimensional shape-controlled manufacturing can accurately define particle geometry via various patterning techniques. However, to date, shape-controlled manufacturing has been primarily focused on the preparation of monocomponent polymeric colloids, and its application toward multicomponent inorganic particles has yet to be demonstrated.[15,46−53]

Inorganic colloids can offer several advantages in sensing and optical applications.[54−56] They can incorporate multiple oxide and nitride layers with desired dielectric constants for selective photonic waveguiding, or contain nanostructured metallic interfaces for plasmonic sensing and detection. Moreover, metallic and oxide colloids can present a variety of organic and biological self-assembled monolayers on their sides, making such particles ideal building blocks in ligand-specific self-assembly studies. Therefore, a universal technique that provides simple access to fully inorganic, nonspherical, and multicomponent particles with precisely controlled composition, dimension and geometry is greatly needed. In this study, we demonstrate a new manufacturing protocol that yields anisotropic multicomponent microcolloids with precisely defined geometries and composition, like those shown in

Received: May 3, 2013
Accepted: July 9, 2013
Published: July 9, 2013

   dx.doi.org/10.1021/am401660t | ACS Appl. Mater. Interfaces 2013, 5, 7323−7329

Figure 1. We then present a functionalization strategy that permits facile nonsymmetrical modification of the particle sides

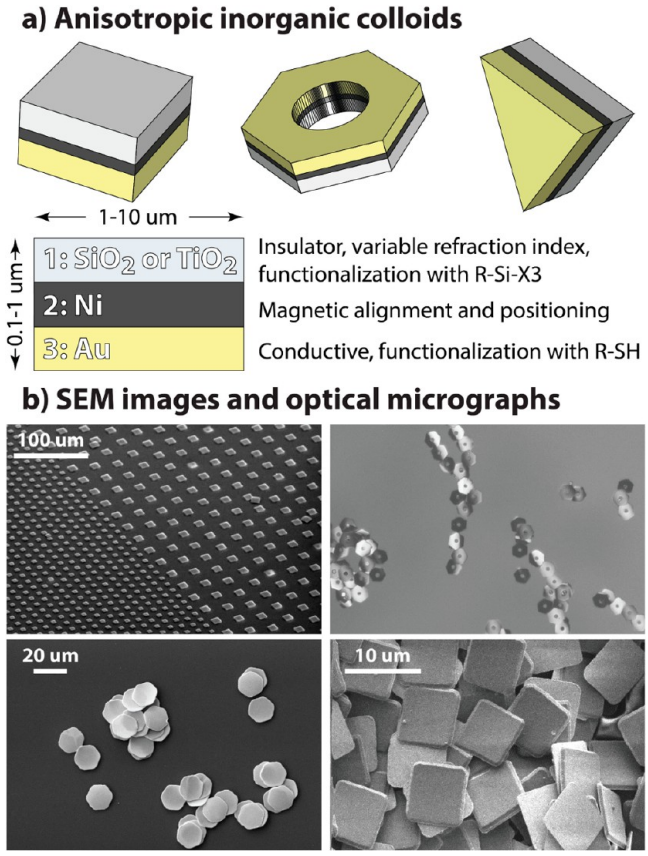

Figure 1. (a) Dimensions and composition of various Janus particles. (b) SEM images of (from top left, counter-clockwise) prepared inorganic particles still attached to the wafer, hexagonal inorganic particles collected after removal from the supporting wafer, collected square inorganic particles, and optical micrographs of hexagonal ring inorganic particles in solution.

with different organic and biological materials. Subsequently, we demonstrate assembly and attachment of the functionalized colloids guided by their surface chemistry and geometry.

RESULTS AND DISCUSSION

Particle Requirements. To use anisotropic colloids in ligand-specific self-assembly, we required particles, which can be orthogonally functionalized with two organic or biological molecules that can act as complementary binding partners. This prerequisite can be achieved by introducing two inorganic thin films that can support different types of organic self-assembled monolayers (SAMs) on two opposite sides of the particle. To facilitate particle handling and separation, we also needed a layer of nonmagnetized ferromagnetic material to control particle position with an external magnetic field. The particle structure that meets these requirements is shown in Figure 1. It includes terminal gold and oxide layers that can support thiolated and silanized organic SAMs. In addition, a thin layer of nickel is positioned in between to provide induced magnetic properties. The colloids bearing a ferromagnetic nickel layer with zero net magnetization will be responsive toward the external magnetic field only, and will not be attracted toward each other in its absence, permitting ligand-specific self-assembly studies.

Particle Fabrication. To manufacture these colloids, we used a combination of two-dimensional micromachining techniques (Figure 2a and b). First, an array of gold−nickel-titanium structures was fabricated on an oxidized silicon wafer using photolithography and physical vapor deposition. These structures were covered with a silicon oxide layer, which was subsequently patterned by reactive ion etching using a positive photoresist as an etching mask. The exposed gold-oxide particles (Au−Ni−Ti−SiO_2) were removed from the wafer by simple sonication in ethanol, due to the low adhesion force between the gold and the native oxide layer on the silicon wafer (Figure 2b).[57] The developed technique inherits all the advantages of photolithography, such as high precision and high throughput, and permits preparation of particles with virtually unlimited geometries and compositions. Notably, the protocol produces ordered arrays of the particles immobilized on a flat surface with their silicon oxide side facing up. Such prearrangement not only significantly alleviates orthogonal functionalization of the particles, but also allows for their selective patterning and labeling through various lithographic techniques, as well as for the precise compartmentalization of the JPs for applications in switchable devices.[10]

Figure 2b (middle) shows an array of Au−Ni−Ti−SiO_2 particles on a silicon wafer after reactive ion etching and positive resist removal. These particles are 8 μm squares comprising layers of gold (500 nm), nickel (75 nm), titanium (75 nm), and silicon oxide (150 nm). The nickel layer gives these particles induced magnetic properties, while the titanium layer serves as an adhesion layer for silicon oxide. As it can be seen from the SEM images, the produced particles were monodisperse and remained intact on the wafer and were not disturbed or shifted during the etching. SEM analysis confirms that all particles were successfully transferred from the wafer to the ethanol solution after sonication. The intrinsic ferromagnetic properties of the internal Ni layer ensured facile separation. Figure 2b (bottom) shows gold-oxide (Au−Ni−Ti−SiO_2) particles on a clean gold surface after they were magnetically separated from the solution. The image clearly shows the difference between the gold and oxide sides and demonstrates uniform morphology and monodisperse size distribution. In ethanol, colloids bearing nonmagnetized nickel layer did not show any tendency toward the aggregation without the external magnetic field. In the presence of the external field, depending on its strength, they were either attracted to its source or demonstrated uniform field-dependent orientation.

The described method relies on a photolithographic alignment to pattern isotropically deposited silicon oxide layer. On advanced instruments, such alignment can be executed with sub-100 nm precision, however, in majority of routine applications it restricts the resolution to a micrometer region. To obviate this limitation we required a method that does not rely on the alignment and, at the same time, produces shape-controlled metal-oxide particles amenable to orthogonal functionalization with at least two different types of organic or biological molecules. Many metal oxides can support well-ordered and robust SAMs. Such metal oxide films can be easily prepared by directly oxidizing anistropically deposited metallic films. Therefore, we decided to substitute an isotropic PECVD deposited silicon oxide layer with an isotropic PVD deposited titania thin film. Such multicomponent metal−metal oxide

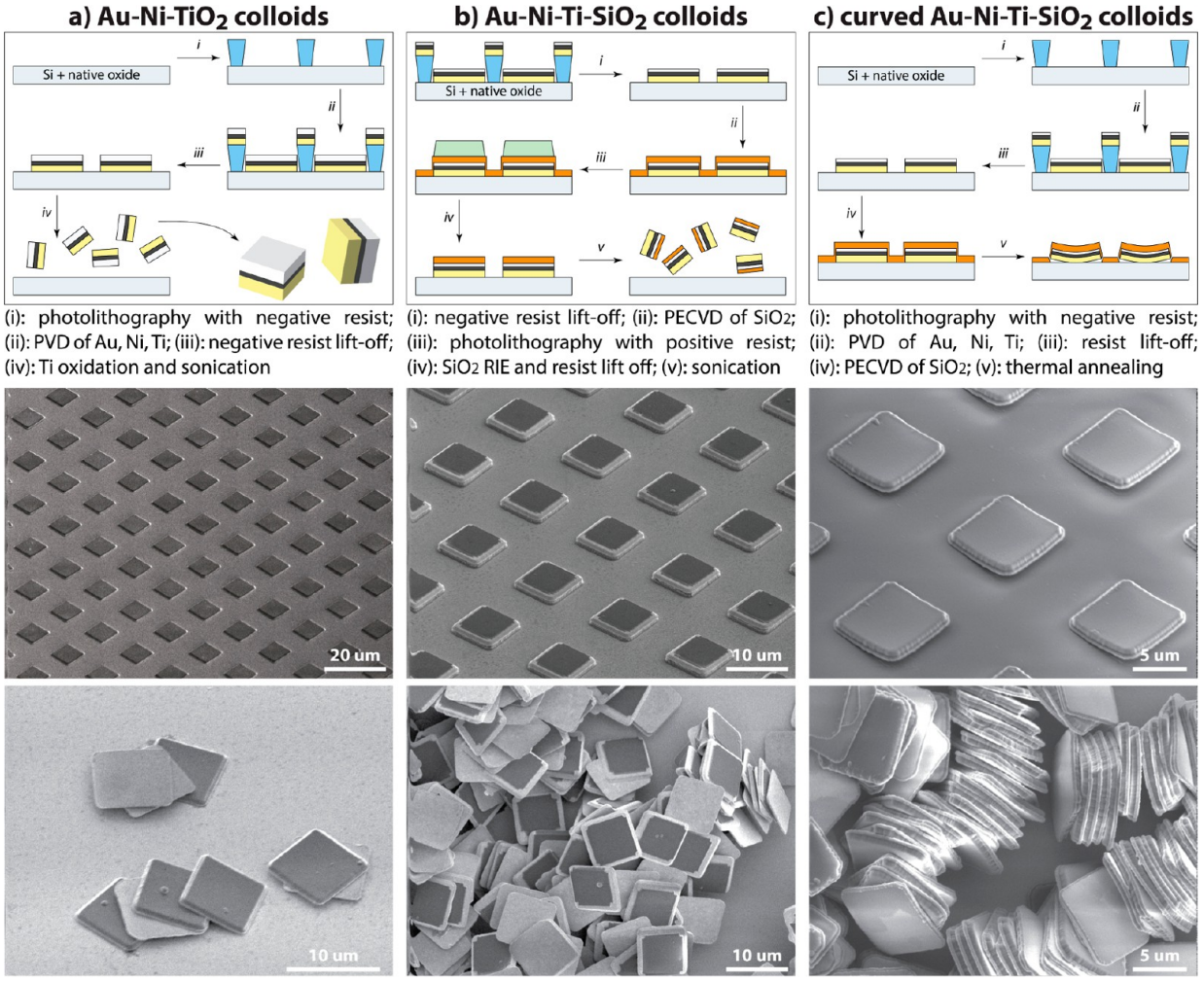

Figure 2. a) (top) Schematic representation of the fabrication of Au−Ni−TiO_2 particles: i) patterning of Si wafer with negative resist and photomask, followed by photolithography ii) electron-beam physical vapor deposition (PVD) of the metals iii) negative resist lift-off iv) oxidation of Ti in O2 plasma, followed by sonication in ethanol to remove the particles from the wafer; (bottom) SEM images of the corresponding 8 μm colloids, on the wafer and removed. **b**) (top) Schematic representation of the fabrication of Au−Ni−Ti-SiO2 particles: i) after repeating the first two steps from the previous scheme, the negative resist was lifted off ii) plasma-enhanced chemical vapor deposition (PECVD) of SiO2 iii) photolithography with a positive resist iv) reactive ion etching (RIE) of SiO2, followed by resist lift-off v) sonication in ethanol to remove the particles from the wafer; (bottom) SEM images of the corresponding 8 μm colloids, on the wafer and removed. **c**) (top) Schematic representation of the fabrication of curved Au−Ni−Ti-SiO2 particles: (i) patterning of Si wafer with negative resist and photomask, followed by photolithography, (ii) electron-beam physical vapor deposition (PVD) of the metals, (iii) negative resist lift-off, (iv) PECVD of SiO2, and (v) thermal annealing; (bottom) SEM images of the corresponding 8 μm colloids, on the wafer and removed.

particles were produced on the silicon wafer by first patterning multilayered metallic structures with the gold−silicon contact on the bottom and a titanium layer on the top, and then by oxidizing the top metallic layer with the oxygen plasma (Figure 2a). This protocol does not require alignment and gives a simple pathway toward gold-oxide (Au−Ni−Ti-TiO_2) particles with precisely controlled morphologies and compositions. Figure 2b (middle) shows 8 μm particles comprising gold (500 nm), nickel (75 nm), and titanium (75 nm) layers on the supporting silicon wafer and on the gold chip. Because this method does not deposit silicon oxide, it can be repeated on the same wafer without complicated cleaning procedures. Using this simplified approach, we have successfully manufactured colloids of more complex shapes (Figure 1), with geometrical features ranging in size from 2 to 20 μm.

The proposed methods are not limited to flat disk-like particles and can be adjusted to manufacture curved colloids. The ability to control the curvature of microscopic multilayered particles has a great potential for the inexpensive scalable manufacturing of micromirror arrays. In our protocol, we used the intrinsic surface-induced stress of particle layers, which remains in some metallic thin films after physical vapor deposition, to control the curvature of the colloids. The observed bending is caused by a mismatch in the thermal coefficients of expansion in the multilayered particles.[58,59] Such residual stress in the nickel films depends on the thickness of the film and on the deposition rate. By increasing the thickness of the nickel layer and by using a higher deposition rate, we were able to produce bent particles comprising gold, nickel, titanium, and silicon oxide layers. Figure 2c shows an array of the particles on the wafer after the silicon oxide deposition. These particles comprise gold (300 nm), nickel (100 nm), titanium (100 nm), and silicon oxide (330 nm) layers. Because of the induced curvature, the particles can be released from the wafer right after the oxide deposition, and no additional photolithographic patterning and etching of the oxide layer is

required. The SEM image of the released particles (Figure 2c, bottom) clearly demonstrates the bent morphology and the difference between the gold and silicon oxide sides. After removal of the particles, the residual oxide layer on the supporting wafer can be etched away and the wafer can be reused.

Orthogonal Functionalization. The goal of this initial study was to develop a manufacturing protocol for the multicomponent shape-controlled colloids and to demonstrate their orthogonal functionalization with different types of organic and biological molecules. Self-assembled monolayers (SAMs) can be effectively used to modify chemical and physical properties of the surfaces supporting them. Oxide and gold can both support well-ordered SAMs of organosilanes and thiols respectively. To orthogonally modify prepared particles with two different SAMs on the opposite sides, the oxide side of the particles was first modified with a fluorinated silane (1*H*,1*H*,2*H*,2*H*-perfluorooctyltriethoxysilane) through a vapor deposition before the particles were released from the substrate. Subsequently, after removing the particles, their gold side was reacted with the solution of mercaptoundecanoic acid (Figure 3). This functionalization protocol was successfully applied with both gold−silicon oxide and gold−titanium oxide particles and produced colloids with opposite hydrophilic and hydrophobic sides. Considering a large variety of commercially and synthetically available thiols and silanes, this strategy can be applied to prepare particles bearing a variety of chemical functional groups on each side. To confirm that the oxide layers on both types of particles can support equivalent SAMs, we compared normalized C1s and F1s X-ray photoelectron spectroscopy (XPS) signals from the wafers with and without particles after they were modified with a fluorinated silane. Figure 3 shows that the fluorine and carbon signals decreased by approximately one-quarter, the area occupied by the particles, after the particles were removed from the wafer, which suggests that the deposited silicon oxide and the oxidized titanium layer can both support SAMs similar to the well-studied monolayers of silanes on a native silicon oxide.

To further demonstrate the successful orthogonal modification of the colloids with dissimilar organics, the C_6F_{13}/COOH-functionalized particles were immobilized on the gold surface, half of which was modified with the amino-terminated SAM. In this experiment, the particle solution was agitated with the gold surface bearing bare and NH_2-terminated regions. The gold substrate was subsequently rinsed with ethanol and dried with filtered nitrogen to remove nonspecifically bound colloids. Figure 3 demonstrates that the majority of the particles adhered to the amino-terminated region of the gold chip. The particles landed on their COOH-terminated side with additional particles adhering to the C_6F_{13}-modified top side of the already immobilized colloids (Figure 3b). This experiment not only demonstrates successful orthogonal functionalization, but also suggests controlled attachment of the colloids to the complementary functionalities on the SAM-modified substrates.

DNA-Based Self-Assembly. The developed functionalization methods were employed in the guided self-assembly of mesoscopic multicomponent colloids. Mesoscopic materials (1−10 μm) have properties different from macroscopic bulk objects, which obey laws of classical mechanics, and from nanomaterials, which primarily consist of surface atoms. The assembly of nanomaterials (100 nm and less) is primarily governed by the chemical functionalities existent on their surfaces; whereas macroscopic bulk objects (100 μm and

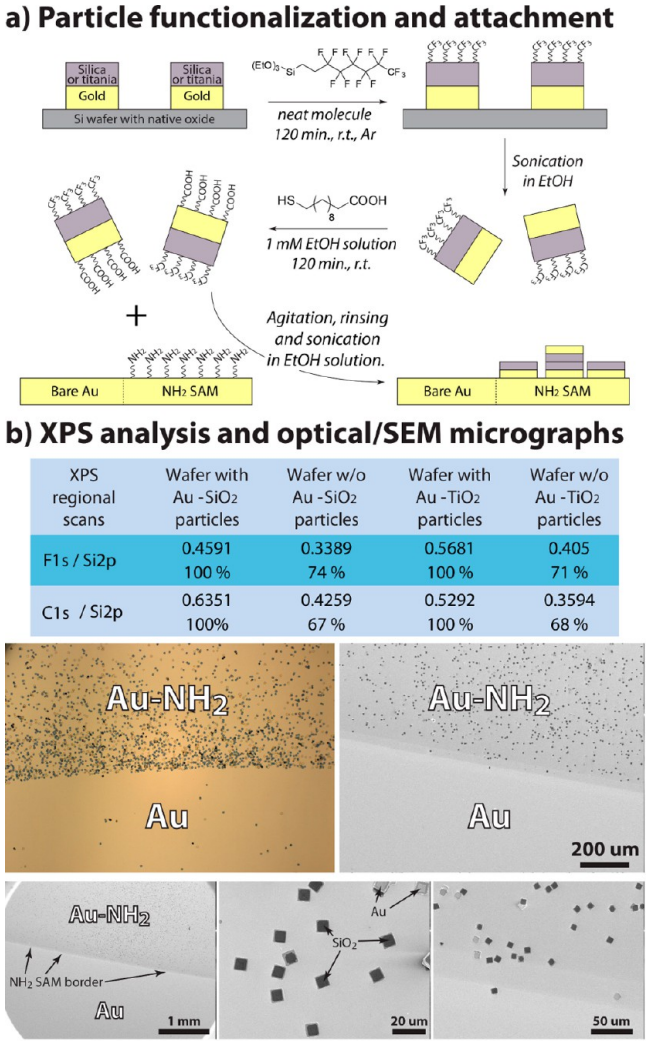

Figure 3. (a) Functionalization protocol: after the particles were fabricated on the wafer and before sonication, the exposed oxide side was reacted with 1*H*,1*H*,2*H*,2*H*-perfluorooctyltriethoxysilane. The particles were then removed from the wafer by sonication in ethanol and collected. Next, the particles were dispersed into a solution containing mercaptoundecanoic acid in ethanol and reacted. After 2 h, the particles were collected, rinsed, and redispersed into a new ethanol solution. The particle solution was agitated with a gold surface bearing bare and NH_2-terminated regions. The gold substrate was subsequently rinsed with ethanol and dried. (b) XPS analysis of the SiO_2 and TiO_2 immobilized SAMs. The similar ~25% decrease in the fluorine and carbon signals (approximately the area occupied by the particles) after the particles were removed from the wafer suggests that the deposited silicon oxide and the oxidized titanium layer can both support SAMs similar to the well-studied monolayers of silanes on a native silicon oxide. Micrographs: Optical and SEM images showing the selective attachment of the COOH-functionalized colloids to the NH_2-terminated SAM on the Au thin film.

more), either organize via lateral capillary actions at liquid−liquid or liquid−air interfaces or do not show any tendencies toward the aggregation.[60] In contrast, the ordered aggregation of mesoscopic colloids is controlled by several equally important interfacial phenomena, such as the geometry and size of the interfacial areas, their roughness, and their chemical properties. Here, we propose a method for studying self-assembly at the mesoscale using our anisotropic inorganic colloids. In this proof-of-concept study, anisotropy in chemical

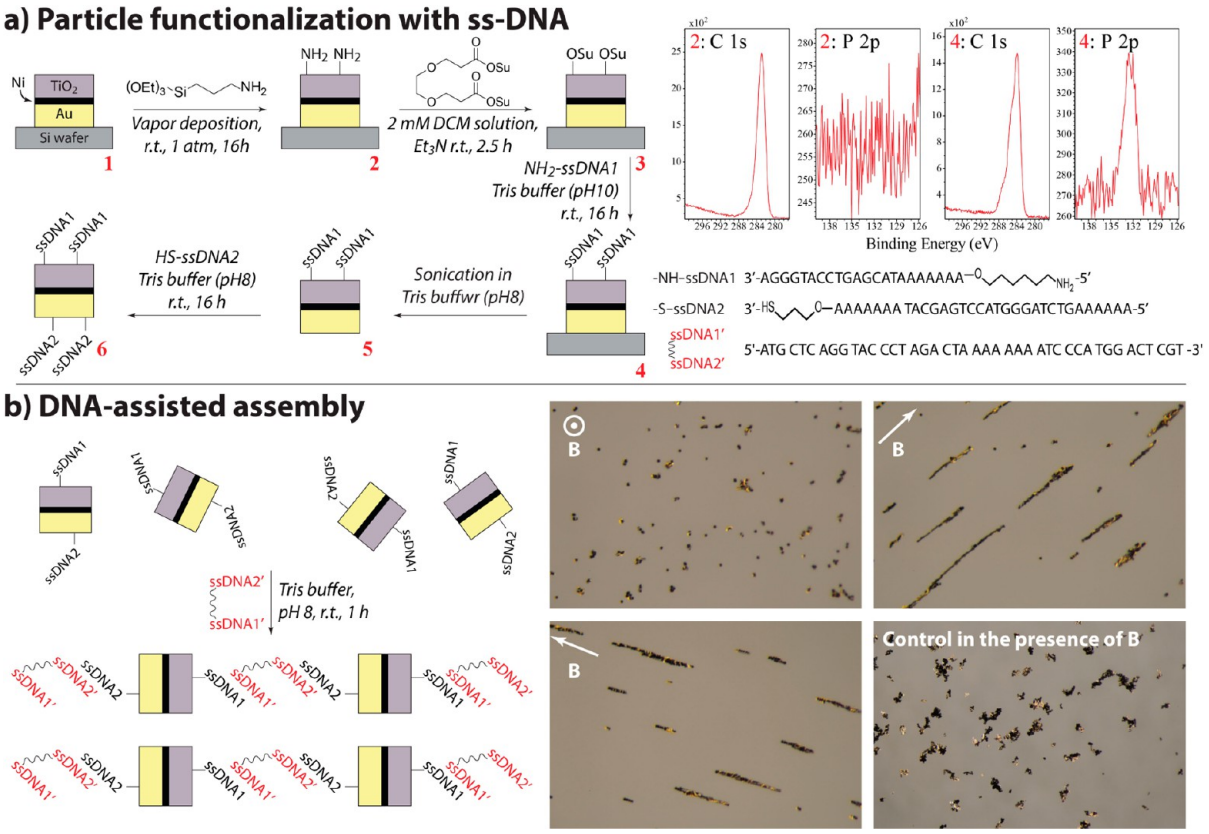

Figure 4. (a) Functionalization protocol: After preparation of Au−Ni−TiO_2 particles on the wafer (**1**), and before their removal, they were exposed to a solution of 3-aminopropyl)triethoxysilane (**2**). Next, the terminal $-NH_2$ group was reacted with bis-NHS ester linker (**3**), and with the single stranded (ss) DNA1 molecule bearing an NH_2 group at the 5′ end (**4**). Following sonication in ethanol to remove the particles from the wafer (**5**), they were exposed to a solution of ss-DNA2 containing a mercapto group at the 3′ end; this yielded colloids functionalized with two different noncomplementary ss-DNA molecules on two opposite sides (**6**). XPS analysis of the TiO_2 immobilized molecules: (2) C 1s peak shows the presence of carbon atoms on the oxide surface of the immobilized particles after reacting with 3-aminopropyl)triethoxysilane; absence of a P 2p peak confirms that there are no phosphorus atoms present on the oxide surface (4) after the reaction with ss-DNA1, the P 2p peak confirms successful attachment of the ss-DNA to the surface of the particles (b) Scheme showing DNA-assisted self-assembly of anisotropic colloids; optical micrographs showing the chain-like aggregates formed from the DNA-functionalized particles in solution. The particle-chains change orientation in the presence of an external magentic field. Vector B indicates the direction of the external magnetic field. A control is shown of particles in free buffer solution (no solution DNA), in the presense of the external magentic field.

properties and shape was used to assemble meso-objects into ordered complex structures. Complementary binding of oligonucleotides provides a simple, yet highly efficient and specific pathway toward guided self-assembly of nano- and microcolloids.[61] We utilized this approach to interconnect disk-like particles using single-stranded DNA molecules anisotropically distributed on particle sides. We demonstrated that gold-oxide Au−Ni−Ti−TiO_2 microparticles, functionalized with two different single-stranded DNAs on the two opposite sides, can assemble into long ordered chains when exposed to a solution of a third DNA, which has complementary sequences to both of the particle-bound DNAs.

DNA-functionalized particles were prepared by modifying their oxide side with (3-aminopropyl)triethoxysilane and by reacting the resulting amino-terminated side with the bis-*N*-hydroxysuccinimide (NHS) ester linker, and with the single stranded (ss) DNA1 molecule bearing an NH_2 group at the 5′-end (Figure 4a). The XPS analysis revealed the presence of the phosphorus atoms, confirming the successful DNA immobilization. Following the oxide functionalization, the particles were removed from the wafer by sonication and their gold side was reacted with a solution of ss-DNA2 containing a mercapto group at the 3′-end. These reactions yielded colloids functionalized with two different noncomplementary single-stranded DNA molecules on two opposite sides. These particles did not show any tendency toward aggregation. The presence of the external magnetic field did not cause aggregation either (Figure 4b control). Following the DNA functionalization, the colloids were incubated at room temperature for 1 h in a 2.5 μM Tris buffer (10 mM, pH8) solution containing the complementary ss-DNA1′-DNA2′ (solution DNA). The presence of the solution DNA allowed for a 14 and 20 base pair hybridizations between ss-DNA1 and ss-DNA1′ and ss-DNA2 and ss-DNA2′ fragments. After exposure to the DNA1′−DNA2′ solution and mild agitation, the particles were observed to form long ordered chain-like structures, which stayed intact even after dispersion in the DNA-free buffer solution (Figure 4b). The alignment of microparticles in the chains was not perfect, presumably because of their large surface area.

The aggregate chain-like macrostructures were predetermined by the particle morphology, due to their disk-like architecture; whereas the ordered aggregation transpired from the side-specific orthogonal functionalization with DNA molecules. Remarkably, no ordered aggregates were formed by the functionalized particles before the addition of the DNA1′−DNA2′ solution (Figure 4b, control). The self-

dx.doi.org/10.1021/am401660t | ACS Appl. Mater. Interfaces 2013, 5, 7323−7329

assembled chains were mechanically stable and aligned themselves along the direction of an external magnetic field because of the presence of a ferromagnetic Ni layer in each particle (Figure 4b, optical micrographs). Such facile manipulation of the aggregates ensures their selective position and uniform orientation in such functional self-assembled devices as colloidal chain-based responsive photonic crystals and self-assembled organic and biomolecular sensors.[62−67]

In this study, we demonstrated that shape-controlled particles, comprising metallic and semiconductor layers on the opposite sides, can be produced by a combination of simple photolithographic and etching techniques. The proposed pathway permits precise control over the particle composition, and, in our future work, will be used used to prepare particles with anisotropic magnetic and/or light reflecting properties. At the same time, the size and the shape of the particles are controlled by the deposition conditions and by the photolithographic pattern (Figure 1). The opposite sides of the particles can be orthogonally functionalized with organic, polymeric, and biological molecules using established surface-grafting protocols to achieve desired physical/chemical properties, while the shape and size of the particles, as well as the composition of the inner core, can all be easily controlled.

MATERIALS AND METHODS

All reagents and solvents were purchased from Sigma-Aldrich and were used as supplied. DNA molecules were ordered from IDT. XPS spectra were recorded on the Kratos Axis Ultra XPS spectrometer equipped with a mono-Al X-ray source. SEM images were recorded on the FEI XL30 SEM-FEG and Zeiss-Auriga microscopes detecting secondary electrons. Optical images were recorded on Zeiss AxioImager microscope and Zeiss Stemi 2000 stereo microscope.

Gold−Silicon Oxide Janus Particles. A silicon wafer was oxidized in oxygen plasma (5 min, 100 W and 6×10^{-1} mbar O_2 pressure), treated with Nanostrip solution (Cyantek co.) for 10 min at 75 °C, washed with DI water, and blow dried with nitrogen. Futurex NR9-1500PY negative photoresist was spun on the wafer at 4000 rpm for 40 s. The resulting substrate was patterned using photolithography and developed in RD6 developer (Futurex) for 11 s. The wafer was treated with oxygen plasma for 45 s to remove undeveloped resist. Layers of gold (500 nm, 5 Å/s), nickel (75 nm, 0.8 Å/s), and titanium (75 nm, 2 Å/s) were evaporated on the patterned wafer in an electron-beam metal evaporator. Subsequently, the negative photoresist was lifted off in RR4 resist remover (Futurex) at 55 °C. The substrate was briefly (10 s) immersed in acetone (55 °C), isopropanol (55 °C), and water (55 °C), and was oven-dried at 115 °C for 5 min. A silicon oxide layer (150 nm) was deposited on the substrate in a plasma enhanced chemical vapor deposition system (PECVD) at 250 °C. Subsequently, the substrate was subjected to the photolithographic alignment and patterning with Shipley 1813 positive photoresist. The exposed substrate was developed in MF319 developer for 35 s, rinsed with water, blow dried with nitrogen, and oven-dried. The exposed silicon oxide layer between the metal-oxide structures was dry etched using the reactive ion etching system (see Supporting Information (SI) for complete details). The remaining photoresist was removed from the top of the metal-oxide structures in warm acetone (55 °C, 5 min) and in Nanostrip solution (room temp, 20 s). The resulting wafer bearing metal-oxide structures was dipped in DI water and in isopropanol, and was oven-dried at 110 °C for 2 min. The Au−Ni−Ti−SiO_2 particles were released from the substrate by sonication in ethanol at room temperature for ∼10−15 min.

Gold−Titanium Oxide Janus Particles. A pattern of photoresist was created via the previously described technique. Layers of gold (500 nm, 5 Å/s), nickel (75 nm, 0.8 Å/s), and titanium (75 nm, 2 Å/s) were evaporated on the patterned wafer. After the lift-off of the photoresist, the titanium layer on the metallic structures was oxidized with oxygen plasma for 10 min at 100 W and 6×10^{-1} mbar O_2 pressure. The gold−titanium oxide particles were released from the substrate by sonication in ethanol at room temp for approximately 10−15 min.

Bent Gold−Silicon Oxide Janus Particles. A pattern of photoresist was created via the previously described technique. Layers of gold (300 nm, 10 Å/s), nickel (100 nm, 2 Å/s), and titanium (100 nm, 5 Å/s) were evaporated on the patterned wafer. Following the lift-off and cleaning procedure, a silicon oxide layer (330 nm) was deposited on the substrate via PECVD at 250 °C. Because of the induced bend in the resulting Au−Ni−Ti-SiO_2 structures, we were able to release them by sonication in ethanol without etching the surrounding silicon oxide layer.

Orthogonal Functionalization of the Gold−Oxide Particles (General Procedure). The gold−oxide Au−Ni−Ti−TiO_2 particles supported on the silicon wafer were exposed to vapors of 1*H*,1*H*,2*H*,2*H*-perfluorooctyltriethoxysilane at room temp for 2 h under argon. The substrate was then left to cure at room temp for 2 days under argon. The particles were released from the wafer by sonication, and were filtered on the 0.45 μm nylon membrane filter (Whatman), where they were washed several times with water, ethanol, acetone, and hexane. The particles were transferred from the filter to a 20 mL vial, and their gold side was reacted with 1 mM ethanol solution of mercaptoundecanoic acid for 2 h at room temp. Subsequently, they were collected and held on the bottom of the vial with a magnet, while they were washed several times with ethanol.

Orthogonal Functionalization of Gold−Oxide Particles with DNA and Self-Assembly. A silicon chip containing gold−titanium oxide particles (8 μm hexagons) was functionalized with 3-aminopropyl triethoxysilane using vapor-phase deposition.[61] The substrate was rinsed with dichloromethane and EtOH and reacted for 2 h 30 min with a 2 mM solution of a Bis-$dPEG_2$-NHS ester in anhydrous dichloromethane. The NHS-functionalized particles were reacted overnight with 25 μM solution of aminated ssDNA1 (sequence 3′-AGGGTACCTGAGCA-TAAAAAAA/5AmMC6/-5′) in a pH 8 10 mM Tris buffer. The DNA-functionalized particles were released from the wafer by sonication in Tris buffer, and were subsequently collected and concentrated using a magnet. Subsequently, the particles were transferred into an Eppendorf tube and reacted overnight with a 25 μM solution of thiolated ssDNA2 (sequence 3′-/3diThioMC3-D/AAAAAAATACGAGTCCATGGGATCTGAAAAAA-5′) and 4.4 mg of dithiothreitol in a pH 8 10 mM Tris buffer. The particles were collected with the magnet, rinsed with Tris buffer (10 mM, pH 8), redispersed in 10 mL of Tris buffer (10 mM, pH 8), and mixed with 1 mL of the 25 μM solution of the complementary ssDNA1′−DNA2′ (sequence 5′-ATGCTCAGGTACCCTAGACTAAA AAAAATCC-CATGGACTCGT-3′). The particles were then incubated in this solution at room temperature for 1 h while mechanically agitated. The incubation resulted in the formation of chain-like aggregates, which were concentrated with the magnet and were redispersed in a DNA-free Tris buffer (10 mM, pH 8).

ASSOCIATED CONTENT

Supporting Information

Detailed experimental procedures. This material is available free of charge via the Internet at http://pubs.acs.org.

AUTHOR INFORMATION

Corresponding Author

*E-mail: alexander.shestopalov@rochester.edu.

Notes

The authors declare no competing financial interest.

ACKNOWLEDGMENTS

We thank Prof Eric J. Toone for his invaluable help in the preparation of this manuscript.

REFERENCES

(1) Walther, A.; Müller, A. H. E. *Chem. Rev.* **2013**, DOI: 10.1021/cr300089t.
(2) Walther, A.; Hoffmann, M.; Mueller, A. H. E. *Angew. Chem., Int. Ed.* **2008**, *47* (4), 711−714.
(3) Glaser, N.; Adams, D. J.; Boeker, A.; Krausch, G. *Langmuir* **2006**, *22* (12), 5227−5229.
(4) Yuet, K. P.; Hwang, D. K.; Haghgooie, R.; Doyle, P. S. *Langmuir* **2009**, *26* (6), 4281−4287.
(5) Anker, J. N.; Behrend, C.; Kopelman, R. *J. Appl. Phys.* **2003**, *93* (10, Pt. 2), 6698−6700.
(6) Anker, J. N.; Behrend, C. J.; Huang, H.; Kopelman, R. *J. Magn. Magn. Mater.* **2005**, *293* (1), 655−662.
(7) Behrend, C. J.; Anker, J. N.; Kopelman, R. *Appl. Phys. Lett.* **2004**, *84* (1), 154−156.
(8) Behrend, C. J.; Anker, J. N.; McNaughton, B. H.; Brasuel, M.; Philbert, M. A.; Kopelman, R. *J. Phys. Chem. B* **2004**, *108* (29), 10408−10414.
(9) Behrend, C. J.; Anker, J. N.; McNaughton, B. H.; Kopelman, R. *J. Magn. Magn. Mater.* **2005**, *293* (1), 663−670.
(10) Nisisako, T.; Torii, T.; Takahashi, T.; Takizawa, Y. *Adv. Mater. (Weinheim, Ger.)* **2006**, *18* (9), 1152−1156.
(11) Howse, J. R.; Jones, R. A. L.; Ryan, A. J.; Gough, T.; Vafabakhsh, R.; Golestanian, R. *Phys. Rev. Lett.* **2007**, *99* (4), 048102/1−048102/4.
(12) Choi, J.; Zhao, Y.; Zhang, D.; Chien, S.; Lo, Y. H. *Nano Lett.* **2003**, *3* (8), 995−1000.
(13) Perro, A.; Reculusa, S.; Ravaine, S.; Bourgeat-Lami, E.; Duguet, E. *J. Mater. Chem.* **2005**, *15* (35−36), 3745−3760.
(14) Bao, Z.; Chen, L.; Weldon, M.; Chandross, E.; Cherniavskaya, O.; Dai, Y.; Tok, J. B. H. *Chem. Mater.* **2002**, *14* (1), 24−26.
(15) Dendukuri, D.; Hatton, T. A.; Doyle, P. S. *Langmuir* **2007**, *23* (8), 4669−4674.
(16) Hong, L.; Cacciuto, A.; Luijten, E.; Granick, S. *Nano Lett.* **2006**, *6* (11), 2510−2514.
(17) Rycenga, M.; McLellan, J. M.; Xia, Y. *Adv. Mater. (Weinheim, Ger.)* **2008**, *20* (12), 2416−2420.
(18) Walther, A.; Mueller, A. H. E. *Soft Matter* **2008**, *4* (4), 663−668.
(19) Panda, P. Ph.D Thesis, Massachusetts Institute of Technology, Cambridge, MA, 2012.
(20) Paunov, V. N.; Cayre, O. J. *Adv. Mater. (Weinheim, Ger.)* **2004**, *16* (9−10), 788−791.
(21) Petit, L.; Manaud, J.-P.; Mingotaud, C.; Ravaine, S.; Duguet, E. *Mater. Lett.* **2001**, *51* (6), 478−484.
(22) Lu, Y.; Xiong, H.; Jiang, X.; Xia, Y.; Prentiss, M.; Whitesides, G. M. *J. Am. Chem. Soc.* **2003**, *125* (42), 12724−12725.
(23) Love, J. C.; Gates, B. D.; Wolfe, D. B.; Paul, K. E.; Whitesides, G. M. *Nano Lett.* **2002**, *2* (8), 891−894.
(24) Hugonnot, E.; Carles, A.; Delville, M.-H.; Panizza, P.; Delville, J.-P. *Langmuir* **2003**, *19* (2), 226−229.
(25) Cayre, O.; Paunov, V. N.; Velev, O. D. *J. Mater. Chem.* **2003**, *13* (10), 2445−2450.
(26) Koo, H. Y.; Yi, D. K.; Yoo, S. J.; Kim, D.-Y. *Adv. Mater. (Weinheim, Ger.)* **2004**, *16* (3), 274−277.
(27) Petit, L.; Sellier, E.; Duguet, E.; Ravaine, S.; Mingotaud, C. *J. Mater. Chem.* **2000**, *10* (2), 253−254.
(28) Gu, H.; Yang, Z.; Gao, J.; Chang, C. K.; Xu, B. *J. Am. Chem. Soc.* **2005**, *127* (1), 34−35.
(29) Pawar, A. B.; Kretzschmar, I. *Macromol. Rapid Commun.* **2010**, *31* (2), 150−168.
(30) Pawar, A. B.; Kretzschmar, I. *Langmuir* **2009**, *25* (16), 9057−9063.
(31) Wang, D.; Moehwald, H. *J. Mater. Chem.* **2004**, *14* (4), 459−468.
(32) Xia, Y.; Yin, Y.; Lu, Y.; McLellan, J. *Adv. Funct. Mater.* **2003**, *13* (12), 907−918.
(33) Yin, Y.; Lu, Y.; Gates, B.; Xia, Y. *J. Am. Chem. Soc.* **2001**, *123* (36), 8718−8729.
(34) Yin, Y.; Lu, Y.; Xia, Y. *J. Am. Chem. Soc.* **2001**, *123* (4), 771−772.
(35) Giersig, M.; Ung, T.; Liz-Marzan, L. M.; Mulvaney, P. *Adv. Mater. (Weinheim, Ger.)* **1997**, *9* (7), 570−575.
(36) Gu, H.; Zheng, R.; Zhang, X.; Xu, B. *J. Am. Chem. Soc.* **2004**, *126* (18), 5664−5665.
(37) Cho, I.; Lee, K. W. *J. Appl. Polym. Sci.* **1985**, *30* (5), 1903−26.
(38) Okubo, M.; Yamashita, T.; Minami, H.; Konishi, Y. *Colloid Polym. Sci.* **1998**, *276* (10), 887−892.
(39) Sheu, H. R.; El-Aasser, M. S.; Vanderhoff, J. W. *J. Polym. Sci., Part A: Polym. Chem.* **1990**, *28* (3), 653−67.
(40) Pfau, A.; Sander, R.; Kirsch, S. *Langmuir* **2002**, *18* (7), 2880−2887.
(41) Teranishi, T.; Inoue, Y.; Nakaya, M.; Oumi, Y.; Sano, T. *J. Am. Chem. Soc.* **2004**, *126* (32), 9914−9915.
(42) Yu, H.; Chen, M.; Rice, P. M.; Wang, S. X.; White, R. L.; Sun, S. *Nano Lett.* **2005**, *5* (2), 379−382.
(43) Gao, X.; Yu, L.; MacCuspie, R. I.; Matsui, H. *Adv. Mater. (Weinheim, Ger.)* **2005**, *17* (4), 426−429.
(44) Reculusa, S.; Poncet-Legrand, C.; Ravaine, S.; Mingotaud, C.; Duguet, E.; Bourgeat-Lami, E. *Chem. Mater.* **2002**, *14* (5), 2354−2359.
(45) Reculusa, S.; Poncet-Legrand, C.; Perro, A.; Duguet, E.; Bourgeat-Lami, E.; Mingotaud, C.; Ravaine, S. *Chem. Mater.* **2005**, *17* (13), 3338−3344.
(46) Herlihy, K. P.; Merkel, T. J.; Brannen, C.; Nunes, J.; DeSimone, J. M. *Polym. Prepr. (Am. Chem. Soc., Div. Polym. Chem.)* **2009**, *50* (1), 78−79.
(47) Merkel, T. J.; Herlihy, K. P.; Nunes, J.; Orgel, R. M.; Rolland, J. P.; DeSimone, J. M. *Langmuir* **2010**, *26* (16), 13086−13096.
(48) Nunes, J. K.; Ertas, M.; Du, L.; DeSimone, J. M. *Chem. Mater.* **2010**, *22* (13), 4069−4075.
(49) Parrott, M. C.; Luft, J. C.; Byrne, J. D.; Fain, J. H.; Napier, M. E.; DeSimone, J. M. *J. Am. Chem. Soc.* **2010**, *132* (50), 17928−17932.
(50) Wang, Y.; Merkel, T. J.; Chen, K.; Fromen, C. A.; Betts, D. E.; DeSimone, J. M. *Langmuir* **2011**, *27* (2), 524−528.
(51) Zhang, H.; Nunes, J. K.; Gratton, S. E. A.; Herlihy, K. P.; Pohlhaus, P. D.; DeSimone, J. M. *New J. Phys.* **2009**, *11* (July), No. 075018.
(52) Dendukuri, D.; Pregibon, D. C.; Collins, J.; Hatton, T. A.; Doyle, P. S. *Nat. Mater.* **2006**, *5* (5), 365−369.
(53) Hernandez, C. J.; Mason, T. G. *J. Phys. Chem. C* **2007**, *111* (12), 4477−4480.
(54) Hartling, T.; Uhlig, T.; Seidenstucker, A.; Bigall, N. C.; Olk, P.; Wiedwald, U.; Han, L.; Eychmuller, A.; Plettl, A.; Ziemann, P.; Eng, L. M. *Appl. Phys. Lett.* **2010**, *96* (18), 183111−3.
(55) Litvinov, J.; Nasrullah, A.; Sherlock, T.; Wang, Y.-J.; Ruchhoeft, P.; Willson, R. C. *PLoS ONE* **2012**, *7* (5), e37440.
(56) Kraus, T.; Malaquin, L.; Schmid, H.; Riess, W.; Spencer, N. D.; Wolf, H. *Nat. Nano* **2007**, *2* (9), 570−576.
(57) Weiss, E. A.; Kaufman, G. K.; Kriebel, J. K.; Li, Z.; Schalek, R.; Whitesides, G. M. *Langmuir* **2007**, *23* (19), 9686−9694.
(58) Atli, K. C.; Franco, B. E.; Karaman, I.; Gaydosh, D.; Noebe, R. D. *Mater. Sci. Eng., A* **2013**, *574* (0), 9−16.
(59) Meisner, L. L.; Lotkov, A. I.; Ostapenko, M. G.; Gudimova, E. Y. *Appl. Surf. Sci.* **2013**, *280* (0), 398−404.
(60) Isaacs, L.; Chin, D. N.; Bowden, N.; Xia, Y.; Whitesides, G. M. *Perspect. Supramol. Chem.* **1999**, *4* (SupramolecularMaterials and Technologies), 1−46.
(61) Milam, V. T.; Hiddessen, A. L.; Crocker, J. C.; Graves, D. J.; Hammer, D. A. *Langmuir* **2003**, *19* (24), 10317−10323.
(62) Ge, J.; Hu, Y.; Yin, Y. *Angew. Chem., Int. Ed.* **2007**, *46* (39), 7428−7431.
(63) Ge, J.; Hu, Y.; Zhang, T.; Huynh, T.; Yin, Y. *Langmuir* **2008**, *24* (7), 3671−3680.
(64) Ge, J.; Lee, H.; He, L.; Kim, J.; Lu, Z.; Kim, H.; Goebl, J.; Kwon, S.; Yin, Y. *J. Am. Chem. Soc.* **2009**, *131* (43), 15687−15694.
(65) Ge, J.; Yin, Y. *J. Mater. Chem.* **2008**, *18* (42), 5041−5045.
(66) Ge, J.; Yin, Y. *Adv. Mater. (Weinheim, Ger.)* **2008**, *20* (18), 3485−3491.
(67) Ge, J.; Yin, Y. *Angew. Chem., Int. Ed.* **2011**, *50* (7), 1492−1522.